GAS HYDRATE DISSOCIATION REGIMES IN HIGHLY PERMEABLE BEDS

G. G. Tsypkin

UDC 532.546:536.421

The gas hydrate decomposition regime in a bed is found, giving rise to two movable phase transition boundaries. A mathematical model of the process is suggested.

In [1] dissociation of a gas hydrate which fully saturates the pore space of the bed was studied. The dissociation front was assumed to separate the hydrate-containing and the water-gas mixture-saturated areas. In [2] it was shown that in a highly permeable bed the minimum temperature occurred at the phase transition front. At substantial pressure drops within the bed the computed equilibrium dissociation temperature may not lie on the equilibrium curve separating the hydrate and the gas-water regions. In this case the gas hydrate decomposition will be accompanied by forming gas and ice. In a bed with a positive initial temperature or in a hydrate-containing bed subjected to heating, apart from the hydrate dissociation front there will be an ice melting surface moving behind the dissociation surface.

In this case the Stefan mathematical model is transformed into a model containing two movable phase transition boundaries which separate the areas saturated with the hydrate, the ice-gas mixture, and the gas-water mixture.

In this article we give a calculation example when the assumption of existence of a dissociation surface separating the areas saturated with hydrate and gas-water mixture does not comply with the dissociation pressure and temperature estimates. A mathematical model of the process that comprises two movable phase transition boundaries is suggested. The problem solution is given in a similarity statement.

1. In [2] a mathematical model was developed for gas hydrate dissociation in hydrate-saturated beds. The model includes mobility of the liquid phase. The decomposition regimes found as a function of the penetrability coefficient can be divided into two classes. In the first case of slightly permeable beds the temperature distribution is monotonic. In the second case when permeability is sufficiently high ($k > 10^{-16}$ m^2) a minimum temperature is found at the gas hydrate dissociation surface. It results from an abrupt pressure drop that enhances the decomposition. Typical pressure and temperature distributions for the latter case are shown in Fig. 1. The dissociation temperature T_* depends primarily on the permeability coefficient, initial temperature of the bed, and pressure at a fixed boundary which simulates a well. In slightly or highly permeable beds the estimated temperature T_* can be lower than the freezing point of water. So, when the computation procedure of [2] is used, for the initial temperature $T_0 = 278$ K, permeability $k = 10^{-11}$ m^2, boundary values of the temperature $T^0 = 373$ K and pressure $P^0 = 1.2 \times 10^6$ Pa we have $T_* = 268$ K. Here even if the near-well area is heated to a high temperature, the dissociation front temperature cannot be prevented from falling, and it drops below the freezing point of water. In nonheated beds with temperatures close to the freezing point of water, a similar trend is observed for rather low permeabilities of the order of 10^{-16} m^2.

Thus, numerical experiments suggest that for a relatively wide parameter range there are hydrate dissociation regimes in a bed with the initial temperature above 273.15 K when the assumption of gas and water production is invalid. In that case it is necessary to assume that hydrate decomposition results in a gas-ice mixture. The heat flux from the surrounding rocks or the well gives rise to an ice melting boundary moving in the dissociation surface direction. Such a process will later be described with a mathematical dissociation model including formation of two unknown mobile phase transition boundaries developed here.

2. As in [1, 2] it will be assumed that the hydrate-containing bed is a porous material fully saturated with gas hydrate and that the thermodynamic conditions at the fixed boundary correspond to the conditions when gas and water are free. We consider the gas hydrate dissociation process within the bed with the parameters, initial and boundary conditions for which the assumption of a dissociation surface separating the hydrate and gas-water regions leads to contradictions. It will be as-

Institute for Mechanics Problems, Russian Academy of Sciences, Moscow, Russia. Translated from Inzhenerno-fizicheskii Zhurnal, Vol. 63, No. 6, pp. 714-721, December, 1992. Original article submitted October 21, 1991.

1062-1025/92/6306-1221$12.50

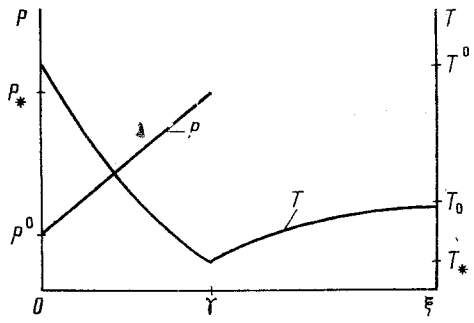

Fig. 1. Typical pressure and temperature distributions at a negative temperature at the dissociation front.

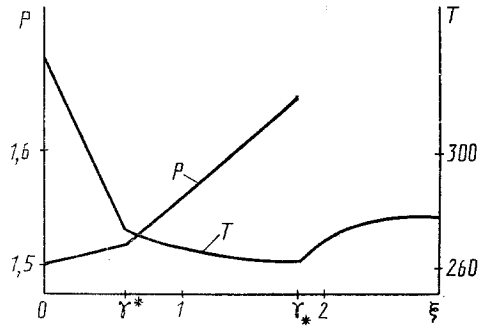

Fig. 2. Plot of temperature and pressure versus the dimensionless similarity variable (T_0 = 277 K, T^0 = 333 K, P^0 = 1.5 MPa, k = 10^{-14} m^2).

assumed in this case that there are two movable phase transition boundaries that separate three areas in which the gas-water mixture occurs in different states. One of the surfaces moving with a large velocity corresponds to the surface where the hydrate dissociates into a gas component and solid water phase. At the other boundary melting of ice occurs.

It will be assumed that the porous skeleton, gas hydrate, and ice are incompressible and immovable, water is an incompressible liquid, gas satisfies the Clapeyron equation, and capillary effects are insignificant. Then, the heat conduction equation holds in the hydrate region

$$\frac{\partial T}{\partial t} = a_1 \Delta T. \tag{1}$$

Here

$$a_1 = \frac{m\lambda_{gh} + (1-m)\lambda_m}{m\rho_{gh}C_{gh} + (1-m)\rho_m C_m}.$$

In the ice-gas region located between the movable boundaries a set of equations is valid, consisting conservation of mass of the gas, the Darcy law, the conservation of energy, and the equation of state of the gas

$$m\frac{\partial}{\partial t}(1-S_i)\rho_g + \operatorname{div}\rho_g \mathbf{v}_g = 0, \quad \mathbf{v}_g = -\frac{kf_g(S_i)}{\mu_g}\operatorname{grad} P, \quad \frac{\partial}{\partial t}(\rho e)_2 + \operatorname{div}(\rho_g h_g \mathbf{v}_g) = \operatorname{div}(\lambda_2 \operatorname{grad} T), \quad P = \rho_g RT. \tag{2}$$

Here $(\rho e)_2 = mS_i\rho_i e_i + m(1-S_i)\rho_g e_g + (1-m)\rho_m e_m$, $\lambda_2 = mS_i\lambda_i + m(1-S_i)\lambda_g + (1-m)\lambda_m$.

It is noteworthy that the ice-saturation function S_i is a constant which can be determined from considerations of a molecular character. Just as in [2], for certainty we consider methane hydrate with the filling degree n = 6 [3]. Then, with molecular masses of methane and water known, it will be found that 1 m^2 of the hydrate, weighing 900 kg, contains 783.87

kg of H_2O. In the solid state this water mass occupies approximately 0.86 of the pore space (in a hydrate-saturated bed). Consequently, $S_i = 0.86$. In the gas-water region located between the fixed wall and the ice melting boundary, a set of equations similar to (2) but taking the liquid phase into consideration is valid

$$m\frac{\partial}{\partial t}(1 - S_w)\rho_g + \operatorname{div}\rho_g \mathbf{v}_g = 0,$$

$$m\frac{\partial}{\partial t}S_w + \operatorname{div}\mathbf{v}_w = 0, \quad \mathbf{v}_g = -\frac{kf_g(S_w)}{\mu_g}\operatorname{grad}P, \quad \mathbf{v}_w = -\frac{kf_w(S_w)}{\mu_w}\operatorname{grad}P, \tag{3}$$

$$\frac{\partial}{\partial t}(\rho e)_3 + \operatorname{div}(\rho_g h_g \mathbf{v}_g + \rho_w h_w \mathbf{v}_w) = \operatorname{div}(\lambda_3 \operatorname{grad}T).$$

Here $(\rho e)_3 = mS_w\rho_w e_w + m(1 - S_w)\rho_g e_g + (1 - m)\rho_m C_m$, $\lambda_3 = mS_w\lambda_w + m(1 - S_w)\lambda_g + (1 - m)\lambda_m$

In the above set of equations the water saturation function S_w is the desired function to be found while solving the problem.

For derivation of the boundary conditions at both movable boundaries use will be made of the universal discontinuity relations for energy and gas and H_2O mass balances and the conditions for the equilibrium phase transitions. Then, under pressure and temperature continuity conditions we have at the gas hydrate dissociation front

$$\begin{aligned}\lambda_-(\operatorname{grad}T)_{n-} - \lambda_+(\operatorname{grad}T)_{n+} - \rho_{g-}h_{g-}(\mathbf{v}_g)_{n-} &= \\ = mV_{*n}\{\rho_{gh}h_{gh} - \rho_{g-}h_{g-}(1 - S_i) - \rho_i h_i S_i\}, \\ \rho_{g-}(\mathbf{v}_g)_{n-} = mV_{*n}\{\rho_{g-}(1 - S_i) - \rho_{g0}\}.\end{aligned} \tag{4}$$

Here $\rho_{g0} = 116.13$ kg/m^3 is the effective gas density in the hydrate-containing region, calculated as the gas mass contained in the hydrate based on the whole pore volume filled with the gas hydrate [2].

The formula of the type given in [4] can be used as the dependence of temperature on pressure

$$\lg P_* = A - \frac{B}{T_*}, \quad A = 5{,}64, \quad B = 1155.$$

The conditions at the ice melting boundary are similar to those at the ice-water phase transition surface in unsaturated ground [5]

$$\begin{aligned}mV_n^*(S_+\rho_i h_i - S_-\rho_w h_w) = \lambda_-(\operatorname{grad}T)_{n-} - \lambda_+(\operatorname{grad}T)_{n+} - \rho_w h_w \mathbf{v}_{w-}, \\ mV_n^*(\rho_i S_+ - \rho_w S_-) = -\rho_w \mathbf{v}_{wn-}, \\ mV_n^*(S_- - S_+) = \mathbf{v}_{gn+} - \mathbf{v}_{gn-}, \quad T^* = F(P^*).\end{aligned} \tag{5}$$

The systems of equations (2), (3) and boundary conditions (4), (5) will be transformed to the systems for temperature T, pressure P, and saturation S using thermodynamic relations and identical transformations. Then, for the gas-ice region we have

$$\begin{aligned}(1_i - S_i)\frac{\partial P}{\partial t} - (1 - S_i)\frac{P}{T}\frac{\partial T}{\partial t} - \\ = \frac{kf_g}{m\mu_g}\operatorname{div}(P\operatorname{grad}P) + \frac{kf_g}{m\mu_g}\frac{P}{T}\operatorname{grad}T\operatorname{grad}P, \\ (\rho C)_2\frac{\partial T}{\partial t} - k\operatorname{div}\left(\frac{f_g}{\mu_g}P\operatorname{grad}P\right) - \\ - \frac{C_V}{R}\frac{P}{T}\frac{f_g}{\mu_g}\operatorname{grad}P\operatorname{grad}T = \operatorname{div}(\lambda_2\operatorname{grad}T).\end{aligned} \tag{6}$$

Here $(\rho C)_2 = mS_i\rho_i C_i + m(1 - S_i)\rho_g C_p + (1 - m)\rho_m C_m$.

In the gas-water region we have

$$m\frac{\partial S_w}{\partial t} = \frac{k}{\mu_w}\operatorname{div}(f_w \operatorname{grad} P),$$

$$(1 - S_w)\frac{\partial P}{\partial t} - P\frac{\partial S_w}{\partial t} - (1 - S_w)\frac{P}{T}\frac{\partial T}{\partial t} =$$

$$= \frac{k}{m\mu_g}\operatorname{div}(f_g P \operatorname{grad} P) + \frac{kf_g}{m\mu_g}\frac{P}{T}\operatorname{grad} P \operatorname{grad} T, \tag{7}$$

$$(\rho C)_3\frac{\partial T}{\partial t} - k\operatorname{div}\left[\left(\frac{f_g}{\mu_g} + \frac{f_w}{\mu_w}\right) P \operatorname{grad} P\right] -$$

$$- \left(\rho_w C_w \frac{f_w}{\mu_w} + \frac{C_V}{R}\frac{f_g}{\mu_g}\frac{P}{T}\right)\operatorname{grad} P \operatorname{grad} T = \operatorname{div}(\lambda_3 \operatorname{grad} T).$$

Here $(\rho C)_3 = mS_i\rho_i C_i + m(1 - S_i)\rho_g C_p + (1 - m)\rho_g C_g$.

Conditions (4) at the dissociation surface reduce to

$$mV_{*n}\rho_{gh} = \lambda_+ (\operatorname{grad} T)_{n+} - \lambda_- (\operatorname{grad} T)_{n-},$$

$$\frac{k}{\mu_g} f_g(S_i)(\operatorname{grad} P)_{n-} = m\left(\frac{\rho_{gh}}{P_*}RT - 1 + S_i\right)V_{*n}, \quad \lg P_* = A - \frac{B}{T_*} \tag{8}$$

At the ice melting boundary we obtain from (5)

$$mS_i\rho_i q^* V_n^* = \lambda_+ (\operatorname{grad} T)_{n+} - \lambda_- (\operatorname{grad} T)_{n-},$$

$$V_n^* = \frac{k}{m\mu_g}\left[\frac{1}{S_- - S_i} f_g(S_-)(\operatorname{grad} P)_{n-} - \frac{1}{S_- - S_i} f_g(S_i)(\operatorname{grad} P)_{n+}\right], \tag{9}$$

$$\left(1 - \frac{S_i}{S_-}\frac{\rho_i}{\rho_w}\right)V_n^* = -\frac{k}{m\mu_w S_-} f_w(S_-)(\operatorname{grad} P)_{n-}, \quad T^* = F(P^*).$$

The last equation of (9) is the dependence of the ice melting temperature on the pressure. Because in highly permeable beds the pressure at the rear melting surface coincides in order of magnitude with the pressure at the fixed wall, $T^* = F(P^0)$ can be assumed. In this estimation the temperature estimation error amounts to hundredths of a degree and can be neglected.

3. We consider gas hydrate dissociation in a bed with the initial temperature T_0 and the pressure P^0 and temperature T^0 at the fixed wall. As in [2], the problem will be solved at small pressure drops. Then, the basic equations can be linearized. The desired functions in the gas-water area will be expressed as nondisturbed quantities and disturbances

$$T = T^0 + T', \; P = P^0 + P', \; S = S^0 + S'.$$

Then, in a linear approximation the set of equations (7) for the gas-water region will become

$$\frac{\partial S'}{\partial t} = \varkappa_w \Delta P',$$

$$\frac{\partial P'}{\partial t} + \delta_3\frac{\partial T'}{\partial t} = \varkappa_3 \Delta P', \tag{10}$$

$$\frac{\partial T'}{\partial t} + \omega_3\frac{\partial P'}{\partial t} = a_3 \Delta T'.$$

Here

$$a_3 = \frac{\lambda_3}{(\rho C)_3}, \quad \omega_3 = -\frac{m(1-S^0)}{(\rho C)_3}, \quad \varkappa_3 = \frac{kP^0}{m(1-S^0)}\left(\frac{f_w}{\mu_w} + \frac{f_g}{\mu_g}\right),$$

$$\delta_3 = -\frac{P^0}{T^0}, \quad \varkappa_w = \frac{kf_w}{m\mu_w}.$$

The value obtained under the condition of an immovable water phase $S^0 = S_i\rho_i/\rho_w$ will be taken as the zero approximation of S^0 for the water saturation function.

A similar set of equations is also produced for the gas-ice region while linearizing about the values at the ice melting surface but with $\varkappa_w \equiv 0$ (the condition of immovable ice). In the region between two immovable boundaries, however, this system can be simplified, if it is borne in mind that the temperature varies between the ice melting point and the dissociation temperature and the pressure ranges from the dissociation pressure to the value at the fixed wall. Then, with the terms of higher order of smallness neglected, we arrive at two independent equations for the pressure and temperature

$$\frac{\partial P'}{\partial t} = \varkappa_2 \Delta P', \qquad \frac{\partial T}{\partial t} = a_2 \Delta T'. \tag{11}$$

Here

$$a_2 = \frac{\lambda_2}{(\rho C)_2}, \quad \varkappa_2 = \frac{kP^0}{m(1-S_i)}\frac{f_g(S_i)}{\mu_g}.$$

We consider the one-dimensional semi-infinite problem. Let T_0, T^0, and P^0 be constants. Then, the problem formulated will have a similarity solution of the form

$$T' = T'(\xi), \quad P' = P'(\xi), \quad S' = S'(\xi),$$

$$X_*(t) = \beta_* \sqrt{t}, \quad X^*(t) = \beta^* \sqrt{t}, \quad \xi = x/\sqrt{t}.$$

The solution in all the three regions can be expressed in terms of the probability integrals.

In the gas-water region ($0 < \xi < \beta^*$), we have

$$P(\xi) = \frac{1}{\alpha_2 - \alpha_1}\left[(1-\alpha_1) b_1 E_1(\xi) - (1-\alpha_2) b_2 E_2(\xi)\right] + P^0,$$

$$T(\xi) = \frac{\omega_3}{\alpha_1 - \alpha_2}\left[b_1 E_1(\xi) - b_2 E_2(\xi)\right] + T^0,$$

$$S(\xi) = \varepsilon\left(\frac{P-P^*}{P^0} - \frac{T-T^*}{T^0}\right) + S_-,$$

$$\alpha_{1,2} = \frac{1}{2}\left(1 + \frac{a_3}{\varkappa_3}\right) \pm \sqrt{\frac{1}{4}\left(1 - \frac{a_3}{\varkappa_3}\right)^2 + \frac{a_3}{\varkappa_3}\delta_3\omega_3},$$

$$b_1 = \frac{1-\alpha_2}{\omega_3}(T^* - T^0) + P^* - P^0, \quad E_1(\xi) = \frac{\operatorname{erf}\left(\frac{\xi}{2}\sqrt{\frac{\alpha_1}{a_3}}\right)}{\operatorname{erf}\left(\frac{\beta^*}{2}\sqrt{\frac{\alpha_1}{a_3}}\right)}, \tag{12}$$

$$b_2 = \frac{1-\alpha_1}{\omega_3}(T^* - T^0) + P^* - P^0, \quad E_2(\xi) = \frac{\operatorname{erf}\left(\frac{\xi}{2}\sqrt{\frac{\alpha_2}{a_3}}\right)}{\operatorname{erf}\left(\frac{\beta^*}{2}\sqrt{\frac{\alpha_2}{a_3}}\right)},$$

$$\varepsilon = \frac{(1-S^0) f_w(S^0)\,\mu_g}{\mu_g f_w(S^0) + \mu_g f_w(S^0)}.$$

In the gas-ice region ($\beta^* < \xi < \beta_*$) the solution has the form

$$T(\xi) = T^* + (T_* - T^*)\frac{\operatorname{erf}\left(\frac{\xi}{2\sqrt{a_2}}\right) - \operatorname{erf}\left(\frac{\beta^*}{2\sqrt{a_2}}\right)}{\operatorname{erf}\left(\frac{\beta_*}{2\sqrt{a_2}}\right) - \operatorname{erf}\left(\frac{\beta^*}{2\sqrt{a_3}}\right)},$$

$$P(\xi) = P^* + (P_* - P^*)\frac{\operatorname{erf}\left(\frac{\xi}{2\sqrt{\varkappa_2}}\right) - \operatorname{erf}\left(\frac{\beta^*}{2\sqrt{\varkappa_2}}\right)}{\operatorname{erf}\left(\frac{\beta_*}{2\sqrt{\varkappa_2}}\right) - \operatorname{erf}\left(\frac{\beta^*}{2\sqrt{\varkappa_2}}\right)}. \tag{13}$$

In the hydrate region ($\beta_* < \xi < \infty$) the temperature distribution is defined by the expression

$$T = (T_* - T_0)\frac{\operatorname{erfc}\left(\frac{\xi}{2\sqrt{a_1}}\right)}{\operatorname{erfc}\left(\frac{\beta_*}{2\sqrt{a_1}}\right)} + T_0. \tag{14}$$

Substituting the solutions (12)-(14) into the boundary conditions at the phase transition fronts gives transcendental equations for the unknown T_*, P_*, β_*, P^*, S_-, and β^*. It should be noted that the solution (13) for the region between two movable boundaries contains unknown functions at both boundaries. Consequently, the sets of equations (8) and (9) comprise one equation set for determination of the seven unknown functions, which should be solved numerically.

4. The calculations were carried out with the following parameters: m = 0.25, R = 520 J/(kg·K), $\rho_w = 10^3$ kg/m^3, $\rho_{gh} = 900$ kg/m^3, $\rho_i = 910$ kg/m^3, $\rho_m = 2\cdot10^3$ kg/m^3, $\mu_g = 1.8 \times 10^{-5}$ Pa·sec, $\mu_w = 1.8 \times 10^{-3}$ Pa·sec, $\lambda_w = 0.58$ W/(m·K), $\lambda_g = 3.4 \times 10^{-2}$ W/(m·K), $\lambda_{gh} = 2.11$ W/(m·K), $\lambda_i = 2.33$ W/(m·K), $\lambda_m = 2$ W/(m·K), $C_i = 2090$ J/(kg·K), $C_w = 4.2 \times 10^3$ J/(kg·K), $C_m = 10^3$ J/(kg·K), $C_{gg} = 2.5 \times 10^3$ J/(kg·K), $C_{ms} = 2 \times 10^3$ J/(kg·K), $q_* = 1.66 \times 10^5$ J/kg, $q^* = 3.34 \times 10^5$ J/kg.

Typical temperature and pressure distributions in the gas hydrate dissociation process producing a two-front structure are shown in Fig. 2. The numerical computations reveal some characteristics of the regime. First, there are three regions different in their phase compositions. Knowledge of the phase composition is of key importance for the development of physical methods used in practice for diagnosing the hydrate-containing bed conditions. It is therefore necessary to distinguish between the cases of hydrate decomposition resulting in formation of solid H_2O and liquid phase. The dimensions of the ice-saturated zone are largely dependent on permeability as well as on pressures and temperatures at the fixed wall. At wall temperatures slightly different from the ice melting point the dimensionless boundary velocity γ^* is essentially smaller than γ_*, and ice occupies nearly the whole hydrate-free region. An increase in the permeability and a pressure decrease in the well enhances the hydrate decomposition, resulting in an increase of the velocity γ_* of the front boundary. A decrease of the permeability or more intensive heating reduces the ice-occupied area. So, the permeability decrease to $k = 10^{-15}$ m^2 gives $\gamma^* = 0.57$, $\gamma_* = 1.04$. As k decreases further, the ice-containing region thickness tends to zero, which is equivalent to the junction of two boundaries and transition to a single-phase regime.

The temperature distribution (Fig. 2) shows that in a two-front regime heat flows mainly from the region before the front even if the stationary wall temperature is low. The rear melting boundary "screens" the heating, and gas hydrate dissociation takes place only due to a pressure drop. It is natural that in the multidimensional problem, heat flux from the surrounding rocks should also be taken into consideration.

The pressure distribution curve has a bend caused by the penetrability jump, and the position of the bend corresponds to the melting ice boundary. The H_2O saturation changes from $S_+ = S_i = 0.86$ to $S_- = 0.49$. In this case the ice interlayer formed there results in a 3.5-fold decrease of the permeability and reduces the amount of water carried out from the well during gas extraction.

It should be noted that the recent generalizations of the mathematical models for gas hydrate dissociation in natural beds were performed because of both the presence of internal thermodynamic inconsistencies and the necessity to consider different factors affecting the physical process [6, 7]. It was demonstrated in [6] that if the gas hydrate in a bed exists together with gas, then for permeability above 10^{-16} m^2 the front dissociation model results in gas hydrate overheating. A

consistent description is achieved by introduction of an extended phase transition region in which gas, water, and hydrate co-exist at thermodynamic equilibrium. In [7] the equilibrium is chosen as the initial existence of the system. In that case the front dissociation regime does not exist at all but dissociation occurs over the whole region. This study is an example illustrating how the inconsistency (water subcooling in the vicinity of the dissociation front) that occurs in a certain parameter region can be eliminated by introducing a movable phase transition boundary.

NOTATION

T, temperature; a, thermal diffusivity; m, porosity; λ, thermal conductivity; ρ, density; C, heat capacity; S, water saturation; v, filtration velocity; k, permeability; f, relative phase permeability; P, pressure; μ, viscosity; e, internal energy density; h, enthalpy density; R, gas constant; q, phase transition heat; V and X(f), velocity and the law of motion of phase transition surfaces; ξ, similarity variable; β, similarity velocity; $\gamma = \beta/(2\sqrt{a_1})$. Subscripts: gh refers to gas hydrate; g, gas; w, water; i, ice; n, normal; +, −, the right- and left-hand values at the boundary; $*$, the value at the dissociation surface; *, the value at the melting surface.

REFERENCES

1. N. V. Cherskii and É. A. Bondarev, Dokl. Akad. Nauk SSSR, **203**, No. 3, 550-552 (1972).
2. G. G. Tsapkin, Inzh.-fiz. Zh., **60**, No. 5, 736-742 (1991).
3. Yu. F. Makogon, Gas Hydrates. Prevention of Their Forming and Use [in Russian], Moscow (1985).
4. É. A. Bondarev, G. D. Babe, A. G. Groisman, et al., Mechanics of Hydrate Formation in Gas Flows [in Russian], Novosibirsk (1976).
5. G. G. Tsypkin, Izv. Akad. Nauk SSSR., Mekh. Zhidk. Gaza, No. 3, 68-73 (1990).
6. A. M. Maksimov and G. G. Tsypkin, Izv. Akad. Nauk SSSR, Mekh. Zhidk. Gaza, No. 3, 84-87 (1990).
7. É. A. Bondarev, A. M. Maksimov, and G. G. Tsypkin, Dokl. Akad. Nauk SSSR, **308**, 575-578 (1989).